ACS OMEGA

http://pubs.acs.org/journal/acsodf

Article

Biogenic Synthesis and Catalytic Efficacy of Silver Nanoparticles Based on Peel Extracts of *Citrus macroptera* Fruit

Prianka Saha, Md. Mahiuddin,* A. B. M. Nazmul Islam, and Bungo Ochiai*

Cite This: *ACS Omega* 2021, 6, 18260−18268

Read Online

ACCESS | Metrics & More | Article Recommendations

ABSTRACT: Biogenically synthesized silver nanoparticles (AgNP) increase the fascination over chemical ones due to their facile and green synthetic process. This study reports the development of an eco-friendly and cost-effective synthesis of AgNPs using an aqueous extract of *Citrus macroptera* fruit peel, an agricultural waste, as a sole agent with both reducing and capping abilities. The formation of AgNPs was verified by the surface plasmon resonance peak at 426 nm in the UV−vis spectrum, X-ray diffraction pattern, and transmission electron micrography images. The AgNPs obtained under the optimized conditions consist of face-centered cubic crystals and spherical morphology with an average size of 11 nm. The AgNPs are coated with phytochemicals in the *C. macroptera* fruit peel extract and are stably dispersible due to their negatively charged nature. The AgNPs effectively catalyzed the reduction of 4-nitrophenol to 4-aminophenol and the degradation of methyl orange and methylene blue in the presence of sodium borohydride. This method employing a fruit peel extract is facile, efficient, eco-friendly, and cost-effective and has potential for industrial green fabrication of AgNPs.

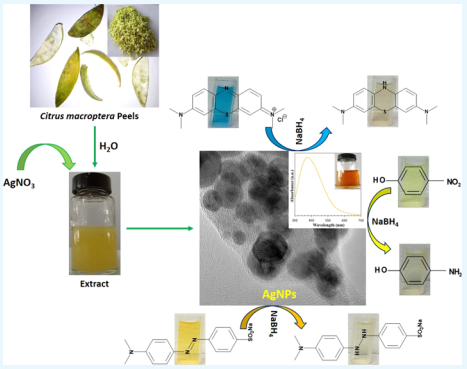

1. INTRODUCTION

Metal nanoparticles (MNPs) are interesting materials due to their substantial impact in the broad area of nanoscience and nanotechnology.[1−5] The size, shape, composition, crystallinity, and structure play pivotal roles in controlling the intrinsic properties of these nanoscopic materials.[6] As a significant member of MNPs, silver nanoparticles (AgNPs) have had a durable impact across a diverse range of fields, including catalysis,[7,8] sensing,[4,9,10] medicine,[11−13] conversion of solar energy,[14,15] and coating.[16]

A variety of methods have been implemented for the synthesis of AgNPs, such as chemical,[17,18] electrochemical,[19] radiation,[20,21] photochemical,[8] Langmuir−Blodgett,[22] and biological[23−25] approaches. Among these methods, the biological approach is advantageous by the three essential green elements, namely, environmentally desirable aqueous systems without requiring organic solvents, naturally abundant reducing and capping agents, and safety.[26,27]

Microorganisms and plant sources are mainly used as reducing and capping agents in the synthesis of AgNPs through a biological approach. The microorganism-based biogenic synthesis produces intracellular and extracellular assemblies containing stabilized NPs under ambient conditions without any auxiliary capping agents.[28] However, the acquiring process of the NPs by intracellular synthesis is difficult, and extracellular synthesis typically requires tedious procedures.[29] In contrast, the plant-source-based biogenic synthesis is advantageous in the simple handling procedures, scalability, and preclusion of cell culture maintenance, and as a result, it is becoming popular.[30]

AgNPs have been synthesized using aqueous extracts of various plant sources including pomegranate peel,[27] Cacumen Platycladi,[28] *Breynia rhamnoides*,[29] *Capsicum annuum* L.,[30] *Alpinia katsumadai*,[31] *Viburnum opulus* L.,[32] *Picea abies* L.,[33] *Thymbra spicata*,[34] *Ocimum sanctum*,[35] *Lonicera japonica*,[36] *Ecklonia cava*,[37] *Ekebergia capensis*,[38] *Abelmoschus esculentus* L.,[39] rice husk,[40] coffee bean,[41] *Cinnamomum camphora*,[42] *Spirulina platensis*,[43] and *Sorghum bran*.[44]

In some cases, edible parts of plant sources are used as the precursors of biogenic synthesis of AgNPs causing competition with food. In contrast, among parts of plant sources, agricultural wastes such as peels, bark, and seeds are economically and ecologically alternative sources. Herein, we focused on the peels of *Citrus macroptera* (*C. macroptera*), a semi-wild species in the Rutaceae family and the citrus genus,[45] which has not been applied for the synthesis of AgNPs to the best of our knowledge. It is also known as Bengali hatkhora, satkara, shatkora, hatxora, cabuyao, Melanesian papeda, or wild

Received: April 23, 2021
Accepted: June 25, 2021
Published: July 9, 2021

https://doi.org/10.1021/acsomega.1c02149
ACS Omega 2021, 6, 18260−18268

Scheme 1. Schematic of the Biogenic Synthesis of AgNPs Using Peel Extracts of *C. macroptera* Fruit

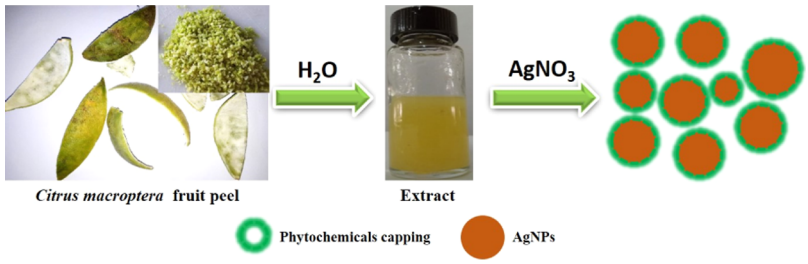

orange. *C. macroptera* is abundantly found in South and Southeast Asia and South Pacific.[46] In Bangladesh, *C. macroptera* grows mostly in the courtyard of the houses and hill tracts of the Sylhet division.[47] The fruit of *C. macroptera* possesses antioxidant, cytotoxic, antimicrobial, antihypertensive, and antipyretic properties, and therefore, not only for edible purpose but it has also been used for the treatment of hypertension, stomach pain, and alimentary disorder.[40,41] The *C. macroptera* fruit contains various biologically active compounds, e.g., β-carotene (ca. 0.22 mg/g), vitamin C (ca. 2.1 mg/g), polyphenols (ca. 0.23 mg gallic acid equivalent/g), and flavonoids (total flavonoid = ca. 0.23 mg-rutin equivalent/g) as major compounds with lesser amounts of tannins and proteins.[47,48] More specifically, its peels contain higher amounts of these active molecules such as polyphenols (ca. 6.2 mg/g), flavonoids (ca. 5.1 mg/g), tannins (ca. 5.9 mg/g), ascorbic acid (ca. 1.2 mg/g), and proteins (ca. 40 μg/g).[47] These compounds serving as antioxidants have the potential to reduce Ag^+ to Ag^0 and presumably realize a cost-effective synthesis of AgNPs in large-scale production.

Organic pollutants, still released from different industries as discharge effluents, are making negative impacts on environments, especially on water.[32,49] These pollutants are harmful to human and animal health because they can cause many diseases including blood disorders, skin irritation, kidney and liver damages, and central nervous system poisoning.[50] The high stability of these compounds is the major challenge to convert them to nontoxic products.[8,34,51] Some nanocatalysts have abilities to catalyze the degradation of these organic pollutants by converting them into nontoxic colorless products through an environmentally friendly process. As a green application of AgNPs, catalytic degradation of organic pollutants is widely investigated.[49,52−54]

In the current study, we utilized aqueous extracts of peel of *C. macroptera* fruit discarded as an agricultural waste for biogenic synthesis of AgNPs. The fruit peel effectively serves as reducing and protecting agents without any auxiliary reagents (Scheme 1). Characterization of the obtained AgNPs were conducted by ultraviolet−visible (UV−vis) spectroscopy, dynamic light scattering (DLS), scanning electron microscopy (SEM), transmission electron microscopy (TEM), X-ray diffraction (XRD), energy-dispersive X-ray spectroscopy (EDX), Fourier transform infrared (FTIR) spectroscopy, and thermogravimetric analysis (TGA). Moreover, we evaluated the catalytic effectiveness of the biogenically synthesized AgNPs by examining the well-reputed 4-nitrophenol (4-NP) reduction to 4-aminophenol (4-AP) and the degradation of organic dyes, namely, methyl orange (MO) and methylene blue (MB), in the presence of sodium borohydride.

2. RESULTS AND DISCUSSION

The AgNPs were synthesized by reacting silver nitrate ($AgNO_3$) with the peel extract of *C. macroptera* at 60 °C for 30 min. The peel extract could act both as a reducing and stabilizing agent. The reaction mixture turned yellowish orange (the inset image in Figure 1). Figure 1 illustrates the UV−vis

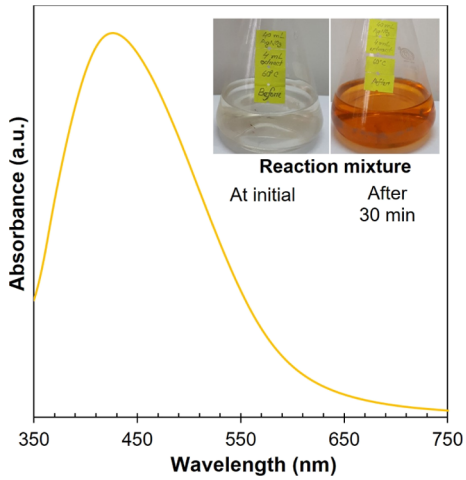

Figure 1. UV−vis spectrum of AgNPs obtained from $AgNO_3$ (2 mM, 40 mL) and the peel extract of *C. macroptera* (4 mL) at 60 °C with optical images of reaction mixtures at the initial stage and after 30 min.

absorption spectrum of the resultant AgNPs. An obvious absorption peak at 426 nm is assignable to a representative surface plasmon resonance (SPR) band of AgNPs, which can be observed between 380 nm and the micrometer range depending on their size and shape, as reviewed by Anker et al.[4]

To propose a suitable synthetic process for the AgNPs, we studied the effects of experimental conditions, namely, temperature, plant extract concentration, $AgNO_3$ concentration, reaction time, and pH. Figure 2 shows the absorption spectra of reaction mixtures obtained by the reaction of the peel extract of *C. macroptera* and $AgNO_3$ at different temperatures for 1 h. As the temperature increased, the intensity of the SPR band increased, indicating the acceleration of the reduction. Beyond 60 °C, a slight red shift of the SPR band was observed in a similar manner to our previous work.[55] The aggregation of the AgNPs could be the reason behind the red shift. The abovementioned result indicates that high-quality AgNPs are obtained at 60 °C.

Figure 3 displays the UV−vis absorption spectra of the reaction mixtures obtained from the reaction using various amounts of the peel extract of *C. macroptera* and 2 mM aqueous solution of $AgNO_3$ (40.0 mL) at 60 °C for 1 h. The

https://doi.org/10.1021/acsomega.1c02149
ACS Omega 2021, 6, 18260−18268

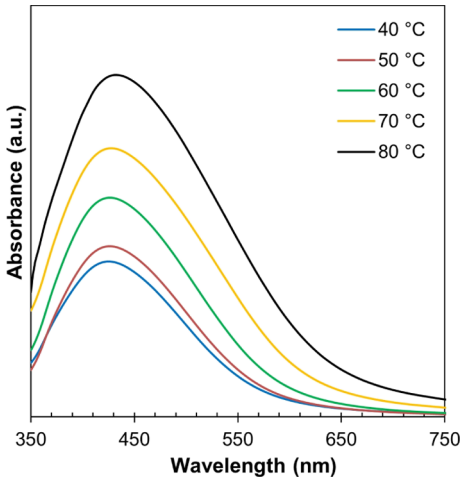

Figure 2. Effect of temperature on absorption spectra of the reaction mixture obtained by reaction of $AgNO_3$ (2 mM, 40 mL) and the peel extract of *C. macroptera* (4 mL) (conditions: pH = 5.5 and 1 h).

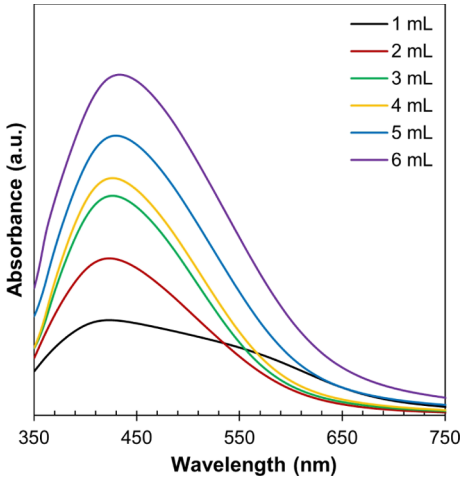

Figure 3. Effect of the amount of peel extract of *C. macroptera* (1−6 mL) on absorption spectra of the reaction mixture of $AgNO_3$ (2 mM, 40 mL) and the peel extract of *C. macroptera* (1−6 mL) (conditions: pH = 5.5, 60 °C, and 1 h).

SPR band was observable in the spectra of the mixtures using more than 2 mL of the extract, while it was unclear using 1 mL of the plant extract. With the increase in the amount of the plant extract, the intensity of the SPR band increased, and the peak tops were shifted to longer wavelengths. The increased intensity of the SPR band indicates the accelerated production and growth of AgNPs, while the red shift originates from the aggregation of AgNPs due to the speedy production and growth of AgNPs in the presence of excess amounts of plant extracts. Up to 4 mL of the plant extract, the red shift was negligible. In contrast, the SPR band of the reaction mixture obtained using 1 mL of the peel extract shows a strong shoulder around 600 nm, suggesting that the insufficient content of phytochemicals to cover the AgNPs resulted in the aggregation. We accordingly considered that the 4 mL amount of the peel extract is optimum.

We next investigated the effect of concentrations of $AgNO_3$ solution. Figure 4 shows the UV−vis absorption spectra of the reaction mixtures obtained from the reaction of the peel extract of *C. macroptera* and $AgNO_3$ at 60 °C for 1 h using different

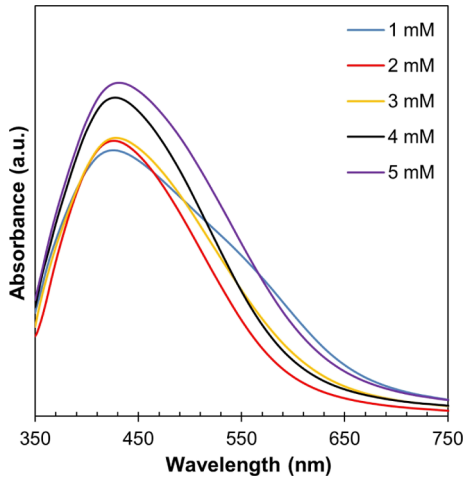

Figure 4. Effect of concentration of $AgNO_3$(1−5 mM, 40 mL) on the absorption spectra of the reaction mixture of $AgNO_3$ (1−5 mM, 40 mL) and the peel extract of *C. macroptera* (4 mL) (conditions: pH = 5.5, 60 °C, and 1 h).

concentrations of $AgNO_3$ solution. The identical color change was observed regardless of the concentrations of $AgNO_3$. With the increase in the concentration of $AgNO_3$, the SPR band intensity increased, indicating the higher production rate of AgNPs due to the presence of a sufficient amount of Ag^+. However, above 3 mM, the SPR band was red-shifted probably by the aggregation of AgNPs due to the excess formation of Ag^0 toward the insufficient amounts of capping substances. On the other hand, with the 2 mM solution, stable AgNPs with a narrower absorption were formed in an identical concentration with those obtained using higher amounts of Ag^+. The mixture obtained using the 1 mM solution of $AgNO_3$ exhibited a broader absorption. Although the reason is unclear, too high amounts of reducing agents in the peel extract toward Ag^+ might lead to too fast reduction before sufficient capping in a similar manner with the aforementioned broadening using too high amounts of the peel extract. We accordingly determined the optimum concentration of $AgNO_3$ to be 2 mM.

The time-dependent UV−vis absorption spectra of the reaction mixtures obtained from the reaction of the peel extract of *C. macroptera* (4.0 mL) and $AgNO_3$ solution (40.0 mL, 2 mM) at 60 °C are demonstrated in Figure 5. The intensity of the SPR band increased over time, indicating the gradual construction of AgNPs. The intensity progressed until 24 h, while the increase in the absorption intensity became slow after 0.5 h. We regard that the reaction time is flexible in obtaining the quality product and can be determined by considering the balance of the yield desired and necessary time.

Figure 6 expresses the pH-dependent absorption spectra of reaction mixtures obtained from the reaction of the peel extract of *C. macroptera* (4 mL) and $AgNO_3$ (40 mL, 2 mM) at 60 °C for 1 h. The pH was adjusted either with HCl or NaOH. The presence of the visible absorptions for all the mixtures indicates the formation of AgNPs under the examined pH conditions. With the increase in pH, the intensity of the SPR band increased, accompanying an increase in the intensity of the shoulder at a longer wavelength region. The pH dependence of the synthesis of the AgNPs with plant sources differs with the plants. For example, acidic conditions are preferable for *Pistia stratiotes*,[56] but basic conditions are suitable for phycocyanin.[57] Although the reason is unclear, unstable dispersion of the

https://doi.org/10.1021/acsomega.1c02149
ACS Omega 2021, 6, 18260−18268

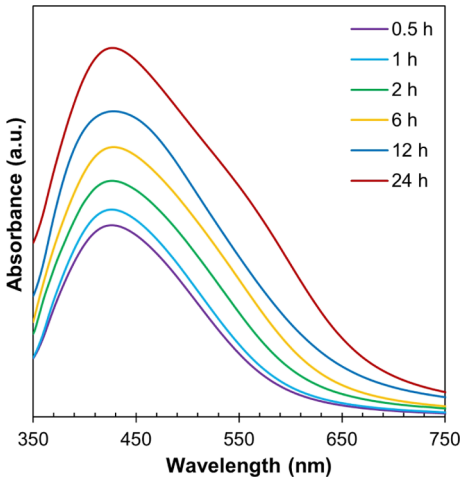

Figure 5. Time course of absorption spectra of the reaction mixture of $AgNO_3$ (2 mM, 40 mL) and the peel extract of *C. macroptera* (4 mL) (conditions: pH = 5.5 and 60 °C).

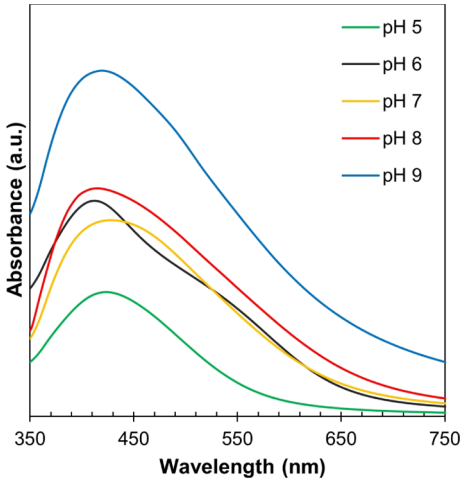

Figure 6. Absorption spectra of the reaction mixture of $AgNO_3$ (2 mM, 40 mL) and the peel extract of *C. macroptera* (4 mL) with different pH values (conditions: 60 °C and 1 h).

capping substances under higher pH conditions is a possible factor, judging from the negative zeta potential of the AgNPs, as described later. The initial pH of the mixture of the peel extract of *C. macroptera* and $AgNO_3$ was approximately 5.5, and AgNPs with good quality were obtained efficiently under the aforementioned conditions without specific control of pH by the addition of an acid or base. To avoid extra chemicals and processes, the reaction only with the peel extract of *C. macroptera* and $AgNO_3$ is more preferable than those with the acid or base.

For these optimizations on the reaction conditions, the AgNPs for further characterization were synthesized using 4 mL of the peel extract and 40 mL of 2 mM $AgNO_3$ solution at 60 °C for 24 h without the addition of other reagents.

2.1. Characterization of the Synthesized AgNPs. In order to investigate the structure of the organic moieties capping the surface of AgNPs, FTIR spectroscopic analysis was conducted. Figure 7 represents the FTIR spectra of the solid contents of the peel extracts and AgNPs. The broad peak at 3393 cm^{-1} observed in both of the spectra was assigned to the stretching vibrations of O−H and N−H bonds. In the

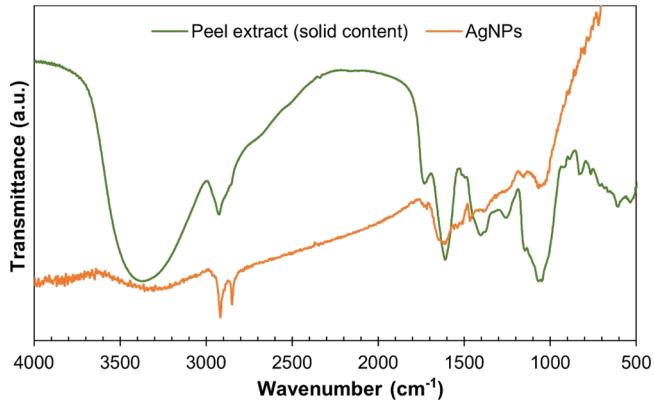

Figure 7. FTIR spectra of the solid component of the peel extract of *C. macroptera* and synthesized AgNPs obtained from $AgNO_3$ (2 mM, 40 mL) and the peel extract of *C. macroptera* (4 mL) at 60 °C for 24 h.

spectrum of AgNPs, a broad shoulder was observed at the lower wavenumber region, which implies the construction of hydrogen bonds through the O−H and N−H bonds within the capping organic molecules and the surface of AgNPs. The bands observed at 2915 and 2847 cm^{-1} were associated with the stretching of aliphatic C−H bonds. Signals were unobservable around 3000 cm^{-1}, indicating the negligible contents of aromatic and alkenyl protons. A small signal at 1715 cm^{-1} corresponds to the stretching vibration of C═O in carboxy and/or ester groups. The broad band at 1604 cm^{-1} is assignable to the stretching vibration of C═O in amide and/or carboxylate moieties and C═C in terpenes, which are found in *C. macroptera* and observed in the FTIR spectrum of the extract.[48] The bands observed at 1455, 1373, and 1046 cm^{-1} are assignable to C−H stretching of methyl groups, C−O−H bending, and C−O stretching, respectively, which are consistent with the plant-derived polysaccharides. These FTIR spectroscopic data indicate that the capping substances consist of amide and hydroxy groups and presumably polysaccharides and carboxy, carboxylate, and/or ester moieties.

The content of the organic moieties capping the AgNPs surface was estimated by TGA (Figure 8). Two stages of weight losses were observed. The first approximately 2% weight loss below 130 °C originates from the evaporation of physisorbed water on the AgNP surface. The second approximately 16% of weight loss that took place at 200−

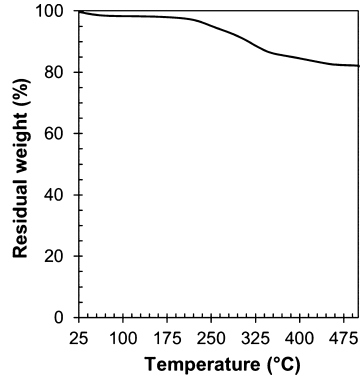

Figure 8. TGA curve of AgNPs obtained from $AgNO_3$ (2 mM, 40 mL) and the peel extract of *C. macroptera* (4 mL) at 60 °C for 24 h.

https://doi.org/10.1021/acsomega.1c02149
ACS Omega 2021, 6, 18260−18268

460 °C is correlated mainly with the degradation of the organic moieties capped on the AgNP surface.

The elemental composition of the AgNPs was evaluated by EDX spectroscopy. Figure 9 illustrates a representative EDX

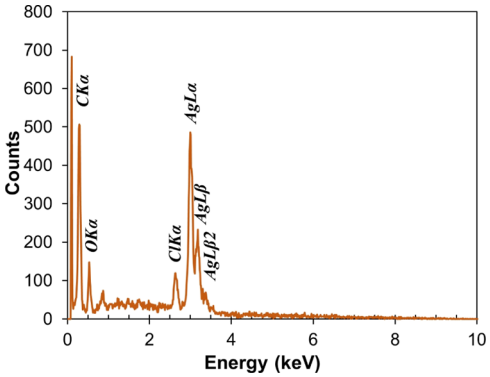

Figure 9. EDX spectrum of AgNPs obtained from $AgNO_3$ (2 mM, 40 mL) and the peel extract of *C. macroptera* (4 mL) at 60 °C for 24 h.

spectrum of AgNPs. Strong signals of Ag (51%) are clearly observable in the spectrum. Other signals of C (32%), O (10%), and Cl (7%) can be attributed to the organic capping layer. The significant intensity of the peaks indicates the presence of a sufficient coating layer on the AgNPs.

Figure 10a shows the SEM image of the AgNPs biogenically synthesized using the peel extract of *C. macroptera*. Almost

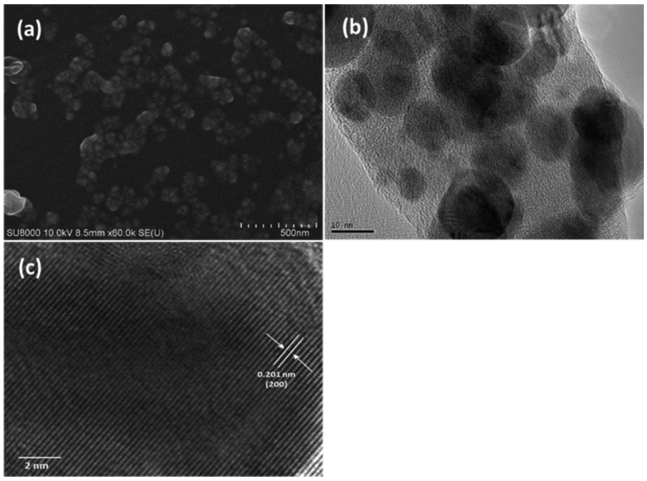

Figure 10. (a) SEM and (b,c) TEM images of AgNPs obtained from $AgNO_3$ (2 mM, 40 mL) and the peel extract of *C. macroptera* (4 mL) at 60 °C for 24 h.

spherical particles with homogeneous morphologies, assignable to AgNPs, were observed. The particles are covered with amorphous substances, assignable to the capping phytochemicals, which aggregate the particles. Figure 10b,c displays the TEM images of AgNPs. The AgNPs are spherical and have an average diameter of 11 nm. Clear lattice fringes are observable in Figure 10c, and an interplanar spacing of 0.201 nm corresponds to the Ag(200) plane.[22,58,59]

Figure 11 represents the XRD pattern of biogenically synthesized AgNPs. Five distinct diffraction peaks were observed at 2θ = 32.41, 38.38, 46.35, 64.68, and 77.67°, corresponding to the lattice planes of (101), (111), (200), (220), and (311), respectively, in Ag(0) having the face-

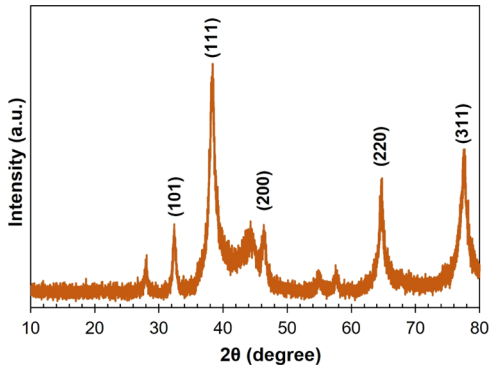

Figure 11. XRD pattern of AgNPs obtained from $AgNO_3$ (2 mM, 40 mL) and the peel extract of *C. macroptera* (4 mL) at 60 °C for 24 h.

centered cubic (fcc) structure (JCPDS file no. 84-0713 and 04-0783). Scherrer's formula was used to estimate the average size of nanocrystallites. The formula is expressed as follows

$$D = k\lambda/\beta \cos\theta$$

where D is the mean size of crystalline domains, k is the dimensionless shape constant (k = 1 for spherical domains), λ is the X-ray wavelength (0.1541 nm), β is the full width at half-maximum, and θ is the diffraction angle corresponding to the lattice plane. The size was calculated to be 12 nm by applying the peaks for the (101) and (220) lattice planes, complying with the average sizes of AgNPs computed from the TEM images. This XRD analysis endorses the hypothesis that single crystallites construct the primary particles of AgNPs.

The pattern lacks diffraction peaks corresponding to oxides but contains a few unassigned peaks (27.94, 44.27, 55.05, and 57.55°) most likely from the organic coating with crystalline phases.[42,44,55,60]

The DLS measurement was executed to obtain the hydrodynamic size of biogenically synthesized AgNPs (Figure 12). An average hydrodynamic diameter (D_h) of 92 nm with

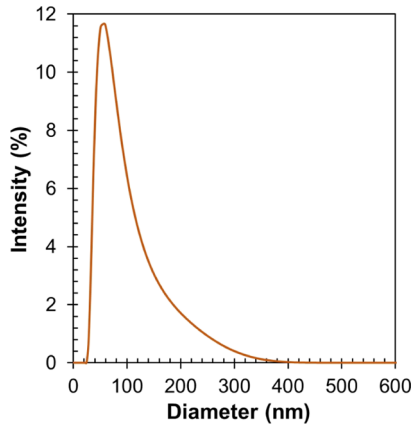

Figure 12. DLS curve of AgNPs obtained from $AgNO_3$ (2 mM, 40 mL) and the peel extract of *C. macroptera* (4 mL) at 60 °C for 24 h.

the polydispersity index value 0.252 is larger than the size of the primary particles observed in the TEM images due to the hydrated layer consisting of swollen phytochemicals capping the surface of the AgNPs similarly to previously reported various AgNPs.[38,39,50] The single-modal DLS profile and D_h comparable to the size of the primary particles suggest that the

https://doi.org/10.1021/acsomega.1c02149
ACS Omega 2021, 6, 18260−18268

nanosized AgNPs are dispersed mostly as single particles without aggregation.

Zeta potential is one of the important indicators to speculate the stability of MNPs. The zeta potential value of the AgNPs is −20.8 mV, and this relatively negative value is an origin of the excellent stability of the AgNPs by the electrostatic repulsion between the particles. Carboxylate moieties are a plausible source of the negative zeta potential and are contained in anionic polysaccharides such as pectin contained commonly in peels of citrus fruits. While complete dispersion stability by electrostatic repulsion typically requires the zeta potentials of > +30 or <−30 mV,[61,62] amphiphiles serving as surfactants may compensate for the insufficient repulsive forces. Various phytochemicals included are also amphiphilic,[47] and thus, a high degree of stability of green synthesized AgNPs could be achieved with zeta potential values not in the abovementioned range.[62,63]

2.2. Catalytic Study. The catalytic activity of the biogenically synthesized AgNPs was performed through the reduction of 4-NP to 4-AP and the degradation of organic dyes (MO and MB) in the presence of sodium borohydride as a reductant.

2.3. Reduction of 4-Nitrophenol to 4-Aminophenol. This reduction of 4-NP to 4-AP is a representative model reaction for evaluating the catalytic performance of different nanoparticles of metals including Ag, Au, Cu, Pt, and Pd.[8] The catalytic reduction of 4-NP was monitored by consumption of the 4-nitrophenolate anion (λ_{max} = 401 nm) through UV spectrophotometry. In the first step, the 4-nitrophenolate anion was formed upon the addition of a freshly prepared aqueous $NaBH_4$ solution to aqueous 4-NP solution (λ_{max} = 317 nm). The characteristic absorption peak instantaneously shifted from 317 to 401 nm accompanied by the change in the color of the solution from light yellow to deep yellow.[29] The advancement of the reduction can be monitored and accessed by observing the decrease in the intensity of the absorption peak of the 4-nitrophenolate anion at 401 nm with the disappearance of the deep yellow color of the 4-nitrophenolate anion. On the addition of the AgNPs, the deep yellow color gradually disappeared, and the intensity of the absorption peak at 401 nm successively decreased. A new peak appeared at 301 nm, and with time, the intensity of the absorption peak increased (Figure 13), indicating the progress of the reduction of 4-NP which was converted to 4-AP. The efficiency of the reduction of 4-NP reached 99.7% within 6 min, which is analogous to the reported catalysis using stable AgNP dispersion having almost identical sizes.[50,53] In the absence of AgNPs, the color and the characteristic absorption peak remain unchanged even after 1 h of the reaction. Without catalysts, the reduction of 4-NP using $NaBH_4$ is thermodynamically feasible but kinetically forbidden.[8,41]

2.4. Degradation of Organic Dyes. Next, degradation of organic dyes by $NaBH_4$ in the presence of AgNPs was explored as an additional model reaction using MO and MB. UV−vis spectroscopy was employed to monitor and access the catalytic degradation process. This reaction of $NaBH_4$ with MO and MB also needs catalysts. Without the AgNPs, the colors of the aqueous solution of dyes were retained over 1 h. When the AgNPs were introduced to the reaction mixture, the reduction of dyes occurred without delay as confirmed by the decoloration of the solutions and the downfall in the intensity of the characteristic absorption peaks. In the case of MO, the solution turned colorless from orange, and meanwhile, the

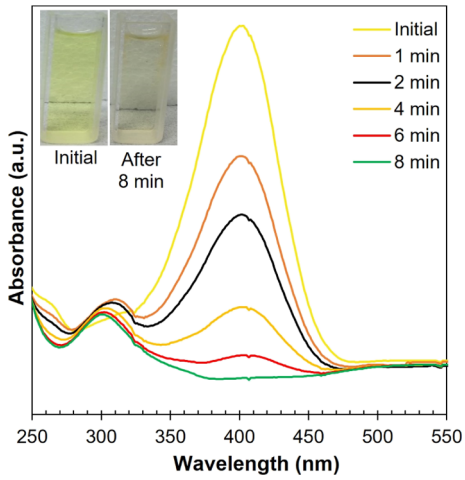

Figure 13. Optical images and time-dependent UV−visible spectra for the catalytic reduction of 4-NP by $NaBH_4$ in the presence of AgNPs. Conditions: [4-NP] = 22 ppm; [catalyst] = 50.1 mg/L; [$NaBH_4$] = 0.025 M; and temperature = 25 °C.

intensity of the absorption peak at 465 nm decreased. This result clearly demonstrates the catalytic activity of the biogenically synthesized AgNPs (Figure 14). MO was quantitatively degraded in 6 min, and this catalytic ability is comparable to that of reported stable AgNP dispersion with almost identical sizes.[64]

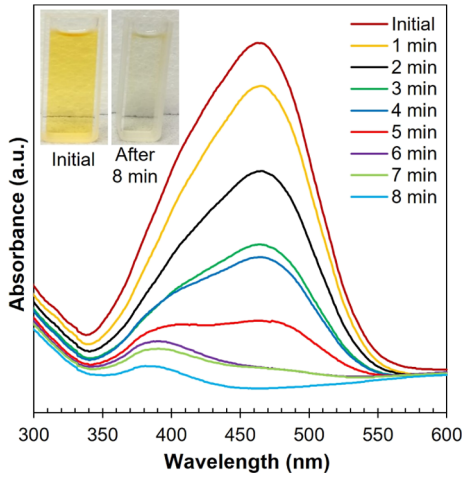

Figure 14. Optical images and time-dependent UV−visible spectra for the catalytic degradation of MO by $NaBH_4$ in the presence of AgNPs. Conditions: [MO] = 15 ppm; [catalyst] = 50.1 mg/L; [$NaBH_4$] = 0.025 M; and temperature = 25 °C.

In the case of MB, the solution turned colorless from blue, and the intensity of the characteristics absorption peak at 665 nm decreased, indicating the catalytic activity of the synthesized AgNPs (Figure 15). The degradation took place in 94.0% efficiency within 6 min, and this catalytic activity is also comparable to that of reported fine AgNPs with almost identical sizes.[51,53]

The specific discoloration by degradation was confirmed by the control experiments because the basicity by $NaBH_4$ may also affect the color of the solutions. The control experiments were conducted at a pH value of 13 using NaOH without AgNPs and $NaBH_4$. The color and characteristic absorption of MO remained unchanged even after 2 h, indicating that pH

https://doi.org/10.1021/acsomega.1c02149
ACS Omega 2021, 6, 18260−18268

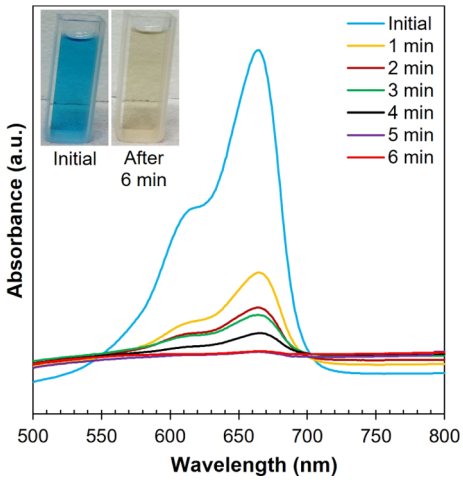

Figure 15. Optical images and time-dependent UV−visible spectra for the catalytic degradation of MB by $NaBH_4$ in the presence of AgNPs. Conditions: [MO] = 10 ppm; [catalyst] = 50.1 mg/L; [$NaBH_4$] = 0.025 M; and temperature = 25 °C.

has no effect on the catalytic degradation of MO. However, the color and absorption of MB changed, but the very low change below 10% is ignorable.

3. CONCLUSIONS

The present study reported a green approach for the synthesis of AgNPs using a peel extract of *C. macroptera* fruit. The procedure is easy, rapid, cost-effective, and eco-friendly and did not require any solvents or reagents except water. In addition, the peel of *C. macroptera* are typically redundant parts, and their use made this synthetic process highly advantageous. The synthetic conditions were optimized using the SPR peak at 426 nm observed in the UV−visible spectra as the index. The AgNPs are spherical and crystalline and consist of the Ag core of 11 nm in size as characterized by the XRD, SEM, TEM, and EDX analyses. The biogenically synthesized AgNPs are capped by phytochemicals stabilizing the dispersion by electrostatic repulsion as confirmed by FTIR spectroscopy, TGA, and DLS measurements. The AgNPs showed excellent catalytic performance toward the reduction of 4-NP to 4-AP and the degradation of MO and MB by $NaBH_4$. This approach is efficient, inexpensive, eco-friendly, and facile and thus has a high probability for industrial applications. This method employing a fruit peel for AgNPs will also be available for efficient utilization of other citrus wastes and possibly applicable to synthesis of other MNPs.

4. EXPERIMENTAL SECTION

4.1. Preparation of the Plant Extract. Fresh satkara fruit (*C. macroptera*) was collected from Bandar Bazar, Sylhet, Bangladesh. The fruit was repeatedly washed with deionized distilled water (DDW). The greenish peel of the fruit was separated and cut into small pieces. The peels (approximately 30 g) and DDW (100 mL) were added in a reaction flask, and then, the mixture was boiled for 10 min. The boiled mixture was cooled down to ambient temperature. The extract was collected by filtration using a filter paper followed by centrifugation at 13,000 rpm. Finally, the extract was preserved in a refrigerator at 4 °C for subsequent use.

4.2. Materials. $AgNO_3$ was purchased from Merck KGaA (Darmstadt, Germany). 4-NP was obtained from Tokyo Chemical Industry Co. Ltd. (Tokyo, Japan). MO, MB, and sodium borohydride were obtained from Kanto Chemical Co. Inc. (Tokyo, Japan). DDW was used throughout the study. All the reagents were used without further purification.

4.3. Measurements. UV−vis spectroscopic analysis was carried out on JASCO (Tokyo, Japan) V-730 series and DR 5000 (HACH, Colorado, USA) spectrometers (resolution = 1 nm and measurement range = 200−800 nm). Quartz cuvettes (height = 4 cm and optical path length = 1 cm) were used. The hydrodynamic size and zeta potential were measured through DLS analysis conducted on a Malvern (Malvern, UK) Zetasizer Nano ZS instrument. FTIR spectra were recorded on a JASCO (Tokyo, Japan) FT/IR-460 plus spectrometer using KBr pellets with a scan rate of 4 cm^{-1} s^{-1} approximately at 25 °C. SEM measurements were conducted on a Hitachi (Tokyo, Japan) SU-8000 microscope at accelerating voltages of 10 and 15 kV. EDX analysis was conducted on a JEOL (Tokyo, Japan) JSM-6510A analytical scanning electron microscope. TEM measurements were conducted on a JEOL (Tokyo, Japan) TEM-2100F field emission electron microscope. XRD analysis was conducted on a Rigaku (Tokyo, Japan) MiniFlex 600 diffractometer with Cu Kα radiation. TGA was carried out on a Seiko Instruments (Tokyo, Japan) TG/DTA 6200 (EXSTER6000) at a heating rate of 10 °C min^{-1} under N_2.

4.4. Biogenic Synthesis of AgNPs. $AgNO_3$ was dissolved in DDW (2 mM, 100 mL) in a volumetric flask before use, and the volumetric flask was covered with carbon paper in order to prevent the autoxidation of silver. The aqueous peel extract of *C. macroptera* (4 mL) and the freshly prepared $AgNO_3$ aq (2 mM, 40 mL) were sequentially added to a conical flask. The mixture was stirred in an oil bath at 60 °C for 30 min with a constant stirring rate. The color of the solution changed from colorless to yellowish orange with the progress of the reaction. The resulting suspension was preserved at ambient temperature for 24 h. The synthesized AgNPs were collected from the reaction mixture through centrifugation at 13,000 rpm for 30 min followed by thorough washing with DDW four times to remove impurities.

4.5. Catalytic Reduction of 4-Nitrophenol to 4-Aminophenol. Aqueous solutions of 0.025 M $NaBH_4$ and 22 ppm 4-NP were used in this catalytic reduction process, and the solutions were stored in a refrigerator at 4 °C before use. The solutions of 4-NP (1.5 mL), $NaBH_4$ (1.5 mL), and colloidal suspension of AgNPs (50.1 mg/L, 200 μL) were mixed in a quartz cuvette to execute the catalytic reduction of 4-NP. The time-dependent decay of 4-NP was monitored by the UV−vis absorbance at 401 nm. The identical procedure was employed to execute the control experiment without AgNPs.

4.6. Degradation of MO and MB. The degradation reactions were conducted by mixing an aqueous solution of MO (15 ppm, 2.5 mL) or MB (10 ppm, 3 mL) and $NaBH_4$ (0.025 M, 1 mL) with the colloidal suspension of AgNPs (50.1 mg/L, 100 μL) in a quartz cuvette. The time-dependent decay of MO and MB was monitored by UV−vis absorbance at 465 and 665 nm, respectively. In both cases, an identical procedure was employed to execute the control experiment without AgNPs.

https://doi.org/10.1021/acsomega.1c02149
ACS Omega 2021, 6, 18260−18268

AUTHOR INFORMATION

Corresponding Authors

Md. Mahiuddin − *Chemistry Discipline, Khulna University, Khulna 9208, Bangladesh; Department of Chemistry and Chemical Engineering, Graduate School of Science and Engineering, Yamagata University, Yamagata 992-8510, Japan;* orcid.org/0000-0002-1195-9159; Email: mahiuddin.chem@ku.ac.bd, tnt11090@st.yz.yamagata-u.ac.jp

Bungo Ochiai − *Department of Chemistry and Chemical Engineering, Graduate School of Science and Engineering, Yamagata University, Yamagata 992-8510, Japan;* orcid.org/0000-0002-4376-8875; Phone: +81-238-26-3092; Email: ochiai@yz.yamagata-u.ac.jp

Authors

Prianka Saha − *Chemistry Discipline, Khulna University, Khulna 9208, Bangladesh*

A. B. M. Nazmul Islam − *Chemistry Discipline, Khulna University, Khulna 9208, Bangladesh*

Complete contact information is available at: https://pubs.acs.org/10.1021/acsomega.1c02149

Author Contributions

This manuscript was written through contributions of all authors. All authors have given approval to the final version of the manuscript.

Notes

The authors declare no competing financial interest.

ACKNOWLEDGMENTS

M.M. gratefully acknowledges the Ministry of Education, Culture, Sports, Science and Technology, Japan, for providing Japanese Government (Monbukagakusho: MEXT) Scholarship. This research receives no external funding.

REFERENCES

(1) Brust, M.; Fink, J.; Bethell, D.; Schiffrin, D. J.; Kiely, C. Synthesis and Reactions of Functionalised Gold Nanoparticles. *J. Chem. Soc., Chem. Commun.* **1995**, *16*, 1655.

(2) Mandal, T. K.; Fleming, M. S.; Walt, D. R. Preparation of Polymer Coated Gold Nanoparticles by Surface-Confined Living Radical Polymerization at Ambient Temperature. *Nano Lett.* **2002**, *2*, 3−7.

(3) Raveendran, P.; Fu, J.; Wallen, S. L. Completely "Green" Synthesis and Stabilization of Metal Nanoparticles. *J. Am. Chem. Soc.* **2003**, *125*, 13940−13941.

(4) Anker, J. N.; Hall, W. P.; Lyandres, O.; Shah, N. C.; Zhao, J.; Van Duyne, R. P. Biosensing with Plasmonic Nanosensors. *Nat. Mater.* **2008**, *7*, 442−453.

(5) Desireddy, A.; Conn, B. E.; Guo, J.; Yoon, B.; Barnett, R. N.; Monahan, B. M.; Kirschbaum, K.; Griffith, W. P.; Whetten, R. L.; Landman, U.; et al. Ultrastable Silver Nanoparticles. *Nature* **2013**, *501*, 399−402.

(6) Soofivand, F.; Mohandes, F.; Salavati-Niasari, M. Simple and Facile Synthesis of Ag2CrO4 and Ag2Cr2O7 Micro/Nanostructures Using a Silver Precursor. *Micro Nano Lett.* **2012**, *7*, 283.

(7) Shiraishi, Y. Colloidal Silver Catalysts for Oxidation of Ethylene. *J. Mol. Catal. A: Chem.* **1999**, *141*, 187−192.

(8) Saha, S.; Pal, A.; Kundu, S.; Basu, S.; Pal, T. Photochemical Green Synthesis of Calcium-Alginate-Stabilized Ag and Au Nanoparticles and Their Catalytic Application to 4-Nitrophenol Reduction. *Langmuir* **2010**, *26*, 2885−2893.

(9) McFarland, A. D.; Van Duyne, R. P. Single Silver Nanoparticles as Real-Time Optical Sensors with Zeptomole Sensitivity. *Nano Lett.* **2003**, *3*, 1057−1062.

(10) Lee, K.-S.; El-Sayed, M. A. Gold and Silver Nanoparticles in Sensing and Imaging: Sensitivity of Plasmon Response to Size, Shape, and Metal Composition. *J. Phys. Chem. B* **2006**, *110*, 19220−19225.

(11) Wright, J. B.; Lam, K.; Hansen, D.; Burrell, R. E. Efficacy of Topical Silver against Fungal Burn Wound Pathogens. *Am. J. Infect. Control* **1999**, *27*, 344−350.

(12) AshaRani, P. V.; Low Kah Mun, G.; Hande, M. P.; Valiyaveettil, S. Cytotoxicity and Genotoxicity of Silver Nanoparticles in Human Cells. *ACS Nano* **2009**, *3*, 279−290.

(13) Chaloupka, K.; Malam, Y.; Seifalian, A. M. Nanosilver as a New Generation of Nanoproduct in Biomedical Applications. *Trends Biotechnol.* **2010**, *28*, 580−588.

(14) Amiri, O.; Salavati-Niasari, M.; Farangi, M.; Mazaheri, M.; Bagheri, S. Stable Plasmonic-Improved Dye Sensitized Solar Cells by Silver Nanoparticles between Titanium Dioxide Layers. *Electrochim. Acta* **2015**, *152*, 101−107.

(15) Amiri, O.; Salavati-Niasari, M.; Farangi, M. Enhancement of Dye-Sensitized Solar Cells Performance by Core Shell Ag@organic (Organic=2-Nitroaniline, PVA, 4-Choloroaniline and PVP): Effects of Shell Type on Photocurrent. *Electrochim. Acta* **2015**, *153*, 90−96.

(16) Kumar, A.; Vemula, P. K.; Ajayan, P. M.; John, G. Silver-Nanoparticle-Embedded Antimicrobial Paints Based on Vegetable Oil. *Nat. Mater.* **2008**, *7*, 236−241.

(17) Van Hyning, D. L.; Zukoski, C. F. Formation Mechanisms and Aggregation Behavior of Borohydride Reduced Silver Particles. *Langmuir* **1998**, *14*, 7034−7046.

(18) Lin, X. Z.; Teng, X.; Yang, H. Direct Synthesis of Narrowly Dispersed Silver Nanoparticles Using a Single-Source Precursor. *Langmuir* **2003**, *19*, 10081−10085.

(19) Yin, B.; Ma, H.; Wang, S.; Chen, S. Electrochemical Synthesis of Silver Nanoparticles under Protection of Poly(N-Vinylpyrrolidone). *J. Phys. Chem. B* **2003**, *107*, 8898−8904.

(20) Li, T.; Park, H. G.; Choi, S.-H. γ-Irradiation-Induced Preparation of Ag and Au Nanoparticles and Their Characterizations. *Mater. Chem. Phys.* **2007**, *105*, 325−330.

(21) Soliman, Y. S. Gamma-Radiation Induced Synthesis of Silver Nanoparticles in Gelatin and Its Application for Radiotherapy Dose Measurements. *Radiat. Phys. Chem.* **2014**, *102*, 60−67.

(22) Zhang, L.; Shen, Y.; Xie, A.; Li, S.; Jin, B.; Zhang, Q. One-Step Synthesis of Monodisperse Silver Nanoparticles beneath Vitamin E Langmuir Monolayers. *J. Phys. Chem. B* **2006**, *110*, 6615−6620.

(23) Akhtar, M. S.; Panwar, J.; Yun, Y.-S. Biogenic Synthesis of Metallic Nanoparticles by Plant Extracts. *ACS Sustainable Chem. Eng.* **2013**, *1*, 591−602.

(24) Mittal, A. K.; Chisti, Y.; Banerjee, U. C. Synthesis of Metallic Nanoparticles Using Plant Extracts. *Biotechnol. Adv.* **2013**, *31*, 346−356.

(25) Xie, J.; Lee, J. Y.; Wang, D. I. C.; Ting, Y. P. Silver Nanoplates: From Biological to Biomimetic Synthesis. *ACS Nano* **2007**, *1*, 429−439.

(26) Mandal, D.; Bolander, M. E.; Mukhopadhyay, D.; Sarkar, G.; Mukherjee, P. The Use of Microorganisms for the Formation of Metal Nanoparticles and Their Application. *Appl. Microbiol. Biotechnol.* **2006**, *69*, 485−492.

(27) Goudarzi, M.; Mir, N.; Mousavi-Kamazani, M.; Bagheri, S.; Salavati-Niasari, M. Biosynthesis and Characterization of Silver Nanoparticles Prepared from Two Novel Natural Precursors by Facile Thermal Decomposition Methods. *Sci. Rep.* **2016**, *6*, 32539.

(28) Huang, J.; Zhan, G.; Zheng, B.; Sun, D.; Lu, F.; Lin, Y.; Chen, H.; Zheng, Z.; Zheng, Y.; Li, Q. Biogenic Silver Nanoparticles by Cacumen Platycladi Extract: Synthesis, Formation Mechanism, and Antibacterial Activity. *Ind. Eng. Chem. Res.* **2011**, *50*, 9095−9106.

(29) Gangula, A.; Podila, R.; M, R.; Karanam, L.; Janardhana, C.; Rao, A. M. Catalytic Reduction of 4-Nitrophenol Using Biogenic Gold and Silver Nanoparticles Derived from Breynia Rhamnoides. *Langmuir* **2011**, *27*, 15268−15274.

(30) Li, S.; Shen, Y.; Xie, A.; Yu, X.; Qiu, L.; Zhang, L.; Zhang, Q. Green Synthesis of Silver Nanoparticles Using Capsicum Annuum L. Extract. *Green Chem.* **2007**, *9*, 852.
(31) He, Y.; Wei, F.; Ma, Z.; Zhang, H.; Yang, Q.; Yao, B.; Huang, Z.; Li, J.; Zeng, C.; Zhang, Q. Green Synthesis of Silver Nanoparticles Using Seed Extract of Alpinia Katsumadai, and Their Antioxidant, Cytotoxicity, and Antibacterial Activities. *RSC Adv.* **2017**, *7*, 39842−39851.
(32) David, L.; Moldovan, B. Green Synthesis of Biogenic Silver Nanoparticles for Efficient Catalytic Removal of Harmful Organic Dyes. *Nanomaterials* **2020**, *10*, 202.
(33) Tanase, C.; Berta, L.; Coman, N. A.; Rosca, I.; Man, A.; Toma, F.; Mocan, A.; Nicolescu, A.; Jakab-Farkas, L.; Biró, D.; et al. Antibacterial and Antioxidant Potential of Silver Nanoparticles Biosynthesized Using the Spruce Bark Extract. *Nanomaterials* **2019**, *9*, 1541.
(34) Veisi, H.; Azizi, S.; Mohammadi, P. Green Synthesis of the Silver Nanoparticles Mediated by Thymbra Spicata Extract and Its Application as a Heterogeneous and Recyclable Nanocatalyst for Catalytic Reduction of a Variety of Dyes in Water. *J. Cleaner Prod.* **2018**, *170*, 1536−1543.
(35) Jain, S.; Mehata, M. S. Medicinal Plant Leaf Extract and Pure Flavonoid Mediated Green Synthesis of Silver Nanoparticles and Their Enhanced Antibacterial Property. *Sci. Rep.* **2017**, *7*, 15867.
(36) Balan, K.; Qing, W.; Wang, Y.; Liu, X.; Palvannan, T.; Wang, Y.; Ma, F.; Zhang, Y. Antidiabetic Activity of Silver Nanoparticles from Green Synthesis Using Lonicera Japonica Leaf Extract. *RSC Adv.* **2016**, *6*, 40162−40168.
(37) Venkatesan, J.; Kim, S.-K.; Shim, M. Antimicrobial, Antioxidant, and Anticancer Activities of Biosynthesized Silver Nanoparticles Using Marine Algae Ecklonia Cava. *Nanomaterials* **2016**, *6*, 235.
(38) Anand, K.; Kaviyarasu, K.; Muniyasamy, S.; Roopan, S. M.; Gengan, R. M.; Chuturgoon, A. A. Bio-Synthesis of Silver Nanoparticles Using Agroforestry Residue and Their Catalytic Degradation for Sustainable Waste Management. *J. Cluster Sci.* **2017**, *28*, 2279−2291.
(39) Mollick, M. M. R.; Rana, D.; Dash, S. K.; Chattopadhyay, S.; Bhowmick, B.; Maity, D.; Mondal, D.; Pattanayak, S.; Roy, S.; Chakraborty, M.; et al. Studies on Green Synthesized Silver Nanoparticles Using Abelmoschus Esculentus (L.) Pulp Extract Having Anticancer (in Vitro) and Antimicrobial Applications. *Arabian J. Chem.* **2019**, *12*, 2572−2584.
(40) Liu, Y.-S.; Chang, Y.-C.; Chen, H.-H. Silver Nanoparticle Biosynthesis by Using Phenolic Acids in Rice Husk Extract as Reducing Agents and Dispersants. *J. Food Drug Anal.* **2018**, *26*, 649−656.
(41) Wang, M.; Zhang, W.; Zheng, X.; Zhu, P. Antibacterial and Catalytic Activities of Biosynthesized Silver Nanoparticles Prepared by Using an Aqueous Extract of Green Coffee Bean as a Reducing Agent. *RSC Adv.* **2017**, *7*, 12144−12149.
(42) Huang, J.; Li, Q.; Sun, D.; Lu, Y.; Su, Y.; Yang, X.; Wang, H.; Wang, Y.; Shao, W.; He, N.; et al. Biosynthesis of Silver and Gold Nanoparticles by Novel Sundried Cinnamomum Camphora Leaf. *Nanotechnology* **2007**, *18*, 105104.
(43) Cepoi, L.; Zinicovscaia, I.; Chiriac, T.; Rudi, L.; Yushin, N.; Miscu, V. Silver and Gold Ions Recovery from Batch Systems Using Spirulina Platensis Biomass. *Ecol. Chem. Eng. S* **2019**, *26*, 229−240.
(44) Njagi, E. C.; Huang, H.; Stafford, L.; Genuino, H.; Galindo, H. M.; Collins, J. B.; Hoag, G. E.; Suib, S. L. Biosynthesis of Iron and Silver Nanoparticles at Room Temperature Using Aqueous Sorghum Bran Extracts. *Langmuir* **2011**, *27*, 264−271.
(45) Dreyer, D. L.; Huey, P. F. Coumarins of Citrus Macroptera. *Phytochemistry* **1973**, *12*, 3011−3013.
(46) Waikedre, J.; Dugay, A.; Barrachina, I.; Herrenknecht, C.; Cabalion, P.; Fournet, A. Chemical Composition and Antimicrobial Activity of the Essential Oils from New Caledonian Citrus Macroptera and Citrus Hystrix. *Chem. Biodiversity* **2010**, *7*, 871−877.
(47) Aktar, K.; Foyzun, T. Phytochemistry and Pharmacological Studies of Citrus Macroptera : A Medicinal Plant Review. *Evidence-Based Complementary Altern. Med.* **2017**, *2017*, 9789802.
(48) Paul, S.; Hossen, M. S.; Tanvir, E. M.; Aminul Isl, M.; Afroz, R.; Ahmmed, I.; Saha, M.; Hua Gan, S.; Khalil, M. I. Antioxidant Properties of Citrus Macroptera Fruit and Its in Vivo Effects on the Liver, Kidney and Pancreas in Wistar Rats. *Int. J. Pharmacol.* **2015**, *11*, 899−909.
(49) Shimoga, G.; Palem, R. R.; Lee, S.-H.; Kim, S.-Y. Catalytic Degradability of P-Nitrophenol Using Ecofriendly Silver Nanoparticles. *Metals* **2020**, *10*, 1661.
(50) Rajamanikandan, R.; Shanmugaraj, K.; Ilanchelian, M. Concentration Dependent Catalytic Activity of Glutathione Coated Silver Nanoparticles for the Reduction of 4-Nitrophenol and Organic Dyes. *J. Cluster Sci.* **2017**, *28*, 1009−1023.
(51) Saha, J.; Begum, A.; Mukherjee, A.; Kumar, S. A Novel Green Synthesis of Silver Nanoparticles and Their Catalytic Action in Reduction of Methylene Blue Dye. *Sustainable Environ. Res.* **2017**, *27*, 245−250.
(52) MeenaKumari, M.; Philip, D. Degradation of Environment Pollutant Dyes Using Phytosynthesized Metal Nanocatalysts. *Spectrochim. Acta, Part A* **2015**, *135*, 632−638.
(53) Shahzad, A.; Kim, W.-S.; Yu, T. Synthesis, Stabilization, Growth Behavior, and Catalytic Activity of Highly Concentrated Silver Nanoparticles Using a Multifunctional Polymer in an Aqueous-Phase. *RSC Adv.* **2015**, *5*, 28652−28661.
(54) Ismail, M.; Khan, M. I.; Khan, S. B.; Akhtar, K.; Khan, M. A.; Asiri, A. M. Catalytic Reduction of Picric Acid, Nitrophenols and Organic Azo Dyes via Green Synthesized Plant Supported Ag Nanoparticles. *J. Mol. Liq.* **2018**, *268*, 87−101.
(55) Mahiuddin, M.; Saha, P.; Ochiai, B. Green Synthesis and Catalytic Activity of Silver Nanoparticles Based on Piper Chaba Stem Extracts. *Nanomaterials* **2020**, *10*, 1777.
(56) Traiwatcharanon, P.; Timsorn, K.; Wongchoosuk, C. Effect of pH on the Green Synthesis of Silver Nanoparticles through Reduction with Pistiastratiotes L. Extract. *Adv. Mater. Res.* **2015**, *1131*, 223−226.
(57) El-Naggar, N. E.-A.; Hussein, M. H.; El-Sawah, A. A. Bio-Fabrication of Silver Nanoparticles by Phycocyanin, Characterization, in Vitro Anticancer Activity against Breast Cancer Cell Line and in Vivo Cytotxicity. *Sci. Rep.* **2017**, *7*, 10844.
(58) Li, B.; Wen, X.; Li, R.; Wang, Z.; Clem, P. G.; Fan, H. Stress-Induced Phase Transformation and Optical Coupling of Silver Nanoparticle Superlattices into Mechanically Stable Nanowires. *Nat. Commun.* **2014**, *5*, 4179.
(59) Girão, A. V.; Pinheiro, P. C.; Ferro, M.; Trindade, T. Tailoring Gold and Silver Colloidal Bimetallic Nanoalloys towards SERS Detection of Rhodamine 6G. *RSC Adv.* **2017**, *7*, 15944−15951.
(60) Vanaja, M.; Annadurai, G. Coleus Aromaticus Leaf Extract Mediated Synthesis of Silver Nanoparticles and Its Bactericidal Activity. *Appl. Nanosci.* **2013**, *3*, 217−223.
(61) Joseph, E.; Singhvi, G. Multifunctional Nanocrystals for Cancer Therapy: A Potential Nanocarrier. *Nanomaterials for Drug Delivery and Therapy*; Elsevier, 2019; pp 91−116.
(62) Sukirtha, R.; Priyanka, K. M.; Antony, J. J.; Kamalakkannan, S.; Thangam, R.; Gunasekaran, P.; Krishnan, M.; Achiraman, S. Cytotoxic Effect of Green Synthesized Silver Nanoparticles Using Melia Azedarach against in Vitro HeLa Cell Lines and Lymphoma Mice Model. *Process Biochem.* **2012**, *47*, 273−279.
(63) Heydari, R.; Rashidipour, M. Green Synthesis of Silver Nanoparticles Using Extract of Oak Fruit Hull (Jaft): Synthesis and In Vitro Cytotoxic Effect on MCF-7 Cells. *Int. J. Breast Cancer* **2015**, *2015*, 1−6.
(64) Joseph, S.; Mathew, B. Microwave-Assisted Green Synthesis of Silver Nanoparticles and the Study on Catalytic Activity in the Degradation of Dyes. *J. Mol. Liq.* **2015**, *204*, 184−191.

https://doi.org/10.1021/acsomega.1c02149
ACS Omega 2021, 6, 18260−18268